Reactive oxygen species-driven mitochondrial injury induces apoptosis by teroxirone in human non-small cell lung cancer cells

JING-PING WANG[1*], CHANG-HENG HSIEH[1*], CHUN-YEN LIU[1], KAI-HAN LIN[1], PEI-TSUN WU[1],
KWUN-MIN CHEN[2] and KANG FANG[1]

Departments of [1]Life Science and [2]Chemistry, National Taiwan Normal University, Taipei 116, Taiwan, R.O.C.

Abstract. Teroxirone as an anticancer agent is used to treat human lung cancer by inducing apoptotic cell death. Previous studies have demonstrated that the status of the tumor suppressor p53 determined the onset of apoptotic cell death in human non-small cell lung cancer cells (NSCLC). In order to further understand the underlying mechanisms of lung cancer, the present study explored the targets of teroxirone. By including antioxidants, the present study analyzed changes in cell proliferation, cell cycle division, mitochondrial membrane potential (MMP), reactive oxygen species (ROS), expression of apoptosis markers and cytochrome c distribution. Subsequent to a 12 h treatment with low concentrations of teroxirone, MMP was suppressed, followed by ROS production and apoptosis in lung cancer cells carrying wild type p53. N-acetylcysteine inhibited apoptotic cell death. The depleted expression of p53, reduction of apoptosis-associated active caspase-3 and poly ADP-ribose polymerase cleavage with resurgence of the pro-survival signal protein kinase B, all demonstrated an antioxidant-mediated reduction of apoptosis by teroxirone. The diminished ROS intensity inhibited the release of mitochondrial cytochrome c and DNA damage. The present study provided evidence that teroxirone treatment induced the ROS-activated intrinsic apoptotic pathway, which led to cell death in human NSCLC cells.

Introduction

Lung cancer remains the leading cause of cancer-associated mortality worldwide, due to poor prognosis, high resistance to therapy and a low survival rate (1). Human non-small cell lung cancer (NSCLC) constitutes ≥80% of patients with lung cancer and includes adenocarcinoma, squamous cell carcinoma and large-cell carcinoma (2). Despite the abundance of available chemotherapeutic approaches, current treatments often lead to severe resistance and side effects (3). Therefore, it is necessary to develop a novel and alternative small molecule drug to provide effective chemotherapy with good efficacy and low toxicity.

Compounds composed of epoxy groups have become an attractive target for chemotherapy development (4). Previously, a triepoxide derivative called teroxirone, proved an effective treatment for patients recovering from leukemia and lymphoma (4,5). Furthermore, a previous study has demonstrated that the tumor suppressor p53 regulates teroxirone-induced apoptosis in human NSCLC cells by damaging cellular DNA (6). Despite the distinctive inhibitory effects demonstrated in cell and animal models, the targets and underlying mechanisms of teroxirone, which lead to p53 activation and final cell growth inhibition, are not yet understood (6). As a regulatory mediator, apoptosis serves to eliminate damaged cells without injuring the surrounding cells (7). Thus, to further understand the detailed mechanisms regarding the onset of apoptosis, the present study assessed mitochondrial functions during p53-dependent apoptosis. The results of the present study demonstrated that teroxirone activated reactive oxygen species (ROS), and that mitochondrial function was impaired as a result of teroxirone treatment, which contributed to cytotoxic effects. Pretreatment of ROS scavengers recovered cell viability by restoring mitochondrial function, reducing DNA damage and attenuating apoptotic characteristics. Thus, the efficacy of teroxirone by apoptotic cell death depended on the generated ROS following the disruption of the membrane potential cascade. The present study also provided further information on the apoptotic mechanisms that may lead to a novel perspective of triepoxides.

Materials and methods

Cell culture. H460 (HTB177™), H1299 (CRL5803™) and A549 (CCL185™) human NSCLC cells were purchased from the American Type Culture Collection (Manassas, VA, USA) and maintained in Dulbecco's modified Eagle's medium (DMEM; Sigma-Aldrich; Merck Millipore, Darmstadt, Germany). All cultured cells were supplemented with

---

Correspondence to: Professor Kang Fang, Department of Life Science, National Taiwan Normal University, 88 Ting-Chou Road, Section 4, Taipei 116, Taiwan R.O.C.
E-mail: kangfang@ntnu.edu.tw

*Contributed equally

L-glutamine, sodium pyruvate and cultured with 10% heat-inactivated fetal bovine serum (FBS; Invitrogen; Thermo Fisher Scientific, Inc., Waltham, MA, USA) in 5% CO_2 at 37˚C. All cell lines were periodically examined using a MycoTect™ kit (Invitrogen; Thermo Fisher Scientific, Inc.), to ensure the absence of mycoplasma contamination.

Chemicals. Dichlorodihydrofluorescein diacetate (DCFH-DA), N-acetylcysteine (NAC), dimethyl sulfoxide (DMSO) and MTT were purchased from Sigma-Aldrich (Merck Millipore). The stock solutions of 10 mM DCFH-DA and NAC as dissolved in DMSO, were passed through a filter with a 0.22 μm pore size (Immobilon; EMD Millipore, Billerica, MA, USA). The synthetic teroxirone, as used previously (6), has a purity of >98%. A stock solution of 10 mM DMSO was stored at -20˚C and freshly dissolved in media prior to use. The penicillin and streptomycin antibiotic mixture, sodium pyruvate and the L-glutamine supplements were supplied by Sigma-Aldrich (Merck Millipore).

Cell viability determination. Cell viability was determined using the trypan blue dye exclusion-staining assay. Briefly, $3x10^5$ cells/well were seeded on a 6-cm dish in DMEM supplemented with 2% FBS. The suspended cells were incubated at 37˚C for 24 h to allow for attachment. Following the indicated duration of exposure time teroxirone, the media was removed and trypsin-EDTA was added in order to suspend the adherent cells. The numbers of cells stained with 0.4% trypan blue were presented as the mean ± standard deviation. The experiments were repeated independently ≥3 times, revealing similar results.

Detection of mitochondrial membrane potential (MMP). Human H460 and A549 NSCLC cells were plated at a density of $3x10^5$ in 6-well plates, allowed to attach overnight and pre-treated with NAC (10 μM) for 2 h at 37˚C, prior to being treated with dimethyl sulfoxide (vehicle control), 2 or 5 μM teroxirone for 12 h at 37˚C. The treated cells were reacted with 2 μM JC-1 for 15 min at 37˚C in a 5% CO_2-supplemented incubator, prior to being washed with PBS and analyzed by flow cytometry (FACSCalibur™; BD Biosciences, Franklin Lakes, NJ, USA) using a 488-nm excitation and data collected at 585 nm wavelength emissions.

Detection of intracellular ROS production. H460 and A549 cells were plated at $3x10^5$ cells/well, attached overnight and treated with 2 or 5 μM teroxirone at 37˚C, followed by staining with 10 μM DCFH-DA for 30 min. The formation of fluorescent-oxidized DCF was monitored using a FACSCalibur™ flow cytometer (excitation at 485 nm, emission at 535 nm). The generated ROS were quantified by evaluating the fluorescence intensity of 10,000 cells using ImageJ software (version 1.45; National Institutes of Health, Bethesda, MD, USA).

Release of cytochrome c. Following the induced release of cytochrome *c* from mitochondria in H460 and A549 cells by treatment with 2 or 5 μM teroxirone, the cells were fixed with 4% formaldehyde, permeabilized and stained with an anti-cytochrome *c* monoclonal antibody (dilution, 1:200; catalog no. 556432; BD Pharmingen; BD Biosciences) at 4˚C

for 18 h. Subsequent to washing with PBS, cells were stained with 10 mM Mitotracker Green (mitochondrial staining; Invitrogen; Thermo Fisher Scientific, Inc.) for 30 min at room temperature, and a secondary antibody conjugated with tetramethylrhodamine (dilution, 1:500; catalog no. T2402, Sigma-Aldrich; Merck KGaA) for cytochrome *c* for 48 h at 4˚C. The slides were counter-stained with 1:2,000 DAPI (Sigma-Aldrich; Merck KGaA) at room temperature for 15 min. The release of cytochrome *c* punctae in cells was quantified using the ImageJ software (version 1.45; National Institutes of Health).

Western blot analysis. Cells treated with teroxirone were washed with PBS and scraped in a lysate buffer substituted with 1% Triton X-100, 150 mM NaCl, 5 mM EDTA, 1% aprotonin, 5 mM phenylmethylsulfonyl fluoride and 10 μg/ml leupeptin as dissolved in 20 mM sodium phosphate buffer. The protein concentrations were determined by a bicinchoninic acid assay (Pierce; Thermo Fisher Scientific, Inc.) and used for western blot analysis. Protein lysates were separated by 10% SDS-PAGE gels and transferred onto nitrocellulose membranes. The blots were blocked for 1 h with 1% skimmed dried milk in Tris-buffered saline (pH 7.6). All antibodies, including secondary antibodies, were used at a 1:2,000 dilution. The primary antibodies used included anti-p53 (catalog no. sc-6243), anti-B-cell lymphoma (Bcl)-2-associated X-protein (Bax; catalog no. sc-0526) (both from Santa Cruz Biotechnology, Dallas, TX, USA), anti-caspase-3 (catalog no. 19677; Proteintech Rosemont, IL, USA), anti-phosphorylated protein kinase B (Akt; catalog no. GTX128414); and anti-Akt (catalog no. GTX121937), anti-poly (ADP-ribose) polymerase (PARP; catalog no. GTX112864), anti-Bcl-2 (catalog no. GTX100064), and anti-cytochrome *c* (catalog no. GTX108585) (all from GeneTex, Irvine, CA, USA). Membranes were then incubated with horseradish peroxidase-conjugated anti-mouse (dilution, 1:3,000; catalog no. F5393) or anti-rabbit IgG (dilution; 1:3,000; catalog no. F0382) (both from Sigma-Aldrich; Merck KGaA) for 1 h at room temperature. Control of protein loading was obtained by probing with an anti-GAPDH antibody (catalog no. GTX100118; GeneTex). The blots were visualized using an enhanced chemiluminescence system (GE Healthcare Life Sciences, Chalfont, UK).

Flow cytometry and cell cycle analysis. A total of $1x10^5$ cells were plated in 12-well plates. For sample preparation, cells were collected, were washed twice with PBS and subsequently preserved with 70% alcohol supplemented with PBS, for 24 h at -20˚C. Immediately prior to analysis, the sample cells were treated with 10 μg/ml propidium iodide (PI; Sigma-Aldrich; Merck Millipore), 10 μg/ml RNase A (ICN Pharmaceuticals, Inc., Costa Mesa, CA, USA) and substituted with PBS, for 30 min in the dark. Data was analyzed by ModFit LT software (version 2.0; BD Biosciences).

Statistical analysis. The data are expressed as the mean ± standard deviation. Statistical differences between two groups were analyzed using one-way analysis of variance and Fisher's least significant difference test. $P < 0.05$ was considered to indicate a statistically significant difference.
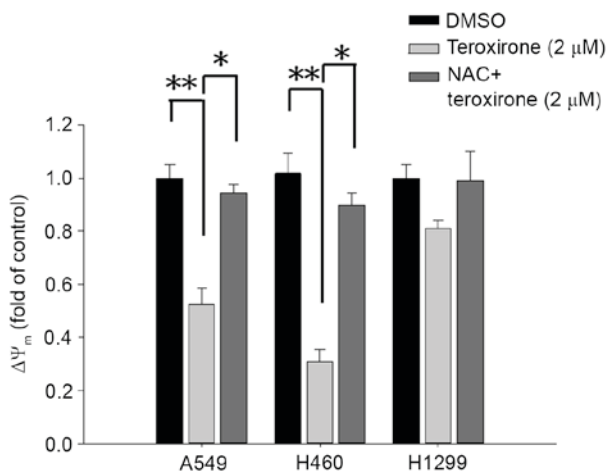
Figure 1. Teroxirone decreased $\Delta\Psi_m$ in NSCLC cells. Cells were seeded onto 6-well plates ($3x10^5$ cells/well). Following 24 h to allow for complete adherence, the cells were treated with teroxirone ($2\ \mu M$) for 12 h, or the cells were pretreated with NAC for 1 h prior to teroxirone treatment. Following 12 h, the cells stained with the fluorescent probe JC-1 were detected by flow cytometry, and the data was converted as fold changes of $\Delta\Psi_m$ relative to the vehicle control (0.2% DMSO). *P<0.05. **P<0.01. $\Delta\Psi$, mitochondrial membrane potential; NSCLC, non-small cell lung cancer; NAC, N-acetylcysteine; DMSO, dimethyl sulfoxide.

Results

Teroxirone induces a decrease in MMP and generates ROS in NSCLC cells. MMP variations were evaluated by incorporating the cells with the voltage-sensitive dye JC-1. The dye aggregates when polarized at high transmembrane potentials emit red fluorescence at 585 nm. The depolarized monomers release green fluorescence at 530 nm as measured by flow cytometry. Treatment with low concentrations of teroxirone resulted in an MMP drop in A549 and H460 cells. The detection of JC-1 fluorescence at higher wavelengths suggests that the induced apoptosis began with disruption of the membrane potential following a 12-h treatment in A549 and H460 cells, whereas H1299 cells were unaffected. Pretreatment of cells with NAC enables cells to recover from membrane potential collapse caused by teroxirone (Fig. 1).

Due to its close association with the leakage of electron transport during MMP decrease, ROS generation was a reasonable selection for investigation in the present study. The stained membrane-impermeable probe DCFH-DA, which was converted into the fluorescent polar derivative DCF, indicated an increase in the level of ROS during flow cytometry analysis. Following MMP disruption, intracellular ROS were identified 18 h following treatment with low concentrations of teroxirone in H460 and A549 cells. Subsequent to a 1-h pretreatment with 10 μM antioxidant NAC, the emitted fluorescence was attenuated that signified the loss of ROS in A549 cells (Fig. 2A). In addition, pretreatment with antioxidant blocked the inhibitory effect on H460 cell growth rate induced by teroxirone (Fig. 2B).

NAC suppressed ROS generation and disrupted cell cycle distribution by teroxirone. Serving a key role in cell death, ROS produced in cells resulted in major changes. The ROS products altered cell growth by influencing cell cycle populations; this was evaluated by PI-stained flow cytometry analysis.
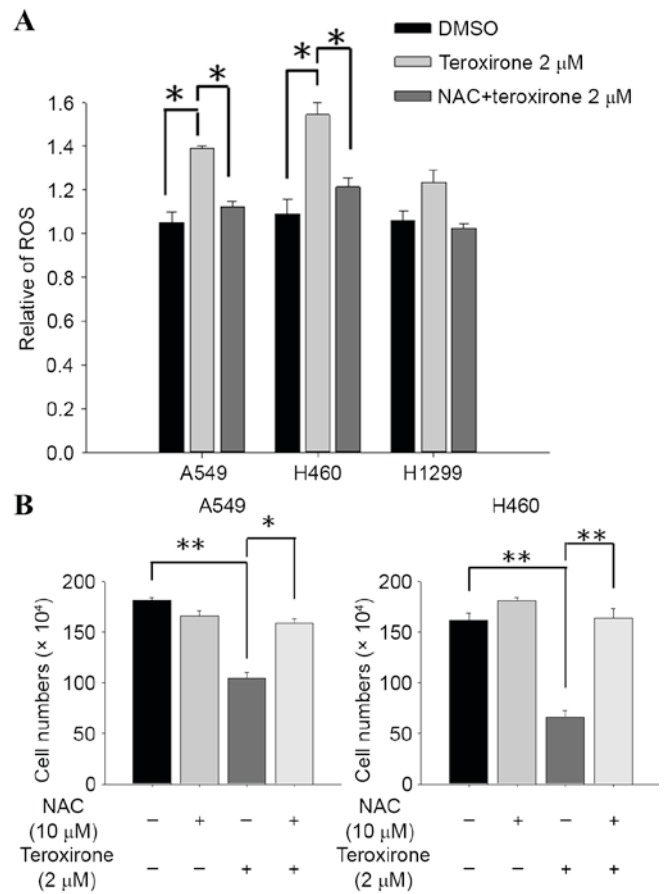

Figure 2. (A) NAC suppressed teroxirone-induced ROS. Cells were seeded onto 12-well plates ($3x10^5$ cells/well). Following 24 h for allowing complete adherence, the cells were pretreated with either NAC (10 μM) for 1 h (+) or the vehicle control (DMSO) (-), followed by treatment with teroxirone ($2\ \mu M$) (+) or 0.2% DMSO as the vehicle control (-) for 18 h. Following treatment, the trypsinized cells were evaluated using flow cytometry, with DCFH-DA as a fluorescent oxidation-sensitive probe. (B) Cell and cell viability determination by teroxirone in A549 and H460 cells. Cells were seeded onto 6-well plates ($3x10^5$ cells/well). Following 24 h to allow for complete adherence, the cells were pretreated with either NAC (10 μM) for 1 h (+) or the vehicle control (DMSO) (-), followed by treatment with teroxirone ($2\ \mu M$) (+) or 0.2% DMSO vehicle control (-) for 24 h. The trypsinized cells were counted using a trypsin-exclusion assay. *P<0.05 and **P<0.01 vs. DMSO control. DCFH-DA, dichlorodihydrofluorescein diacetate; DMSO, dimethyl sulfoxide; ROS, reactive oxygen species; NAC, N-acetylcysteine.

The results revealed that treatment with teroxirone for 24 h induced cell accumulation at the sub-G_1 phase, at the expense of those at G_0/G_1 and S phases, in H460 and A549 cells but not in H1299 cells. Pretreatment with NAC blocked the sub-G_1 phase cell increase that suggested recovery of viable cells as suppressed by ROS (Fig. 3).

Teroxirone induces the p53-dependent apoptosis of NSCLC cells in an ROS-dependent manner. ROS was revealed to induce cell cycle arrest and cell death. Western blot analysis was used to investigate if mitochondrial-mediated apoptosis determinants may be affected by teroxirone. The results demonstrated that treatment of teroxirone for 24 h increased expression levels of intrinsic apoptosis-related markers, including Bax, active caspase-3 and cleaved PARP, alongside p53 activation in A549 (Fig. 4A) and H460 (Fig. 4B) cells.
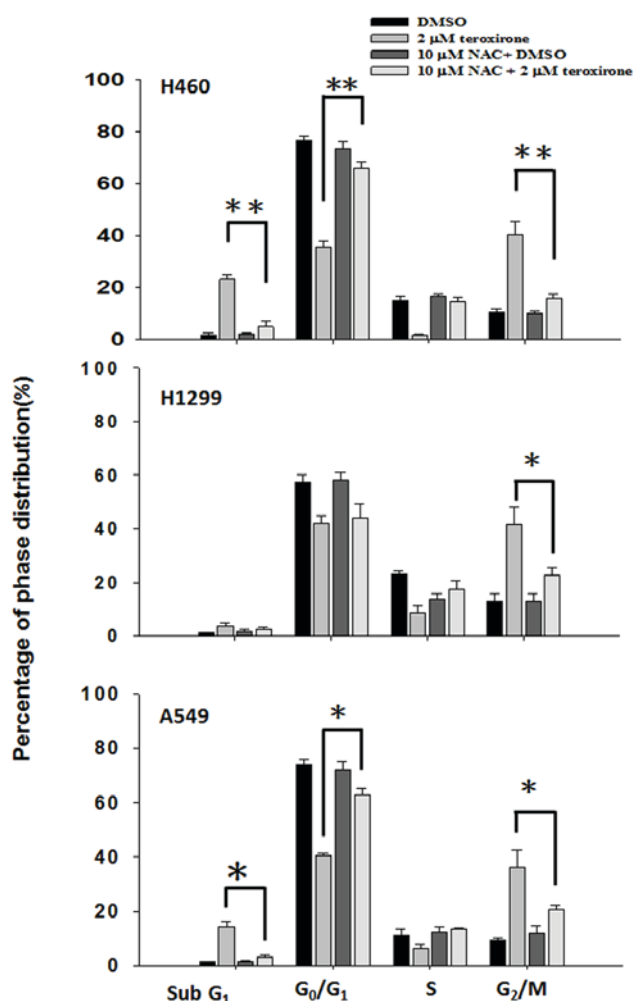
Figure 3. NAC suppressed the effect of ROS generation and disrupted cell cycle distribution of NSCLC cells by teroxirone. Cells were seeded onto 12-well plates (1x10^5 cells/well). Following 24 h to allow for complete adherence, the cells were pretreated with either NAC (10 μM) for 1 h (+) or the vehicle control (DMSO) (-), followed by treatment with teroxirone (2 μM) (+) or 0.2% DMSO vehicle control (-) for 24 h. The collected cells were stained with propidium iodide for phase distribution analysis by flow cytometry. The population distributions following treatment were compared with those of the 0.2% DMSO control. *P<0.05 and **P<0.01 vs. DMSO control; NAC, N-acetylcysteine; ROS, reactive oxygen species; NSCLC, non-small cell lung cancer cells; DMSO, dimethyl sulfoxide.

Furthermore, teroxirone suppressed the expression levels of the proliferation marker Akt, and the mitochondrial anti-apoptotic signal Bcl-2. NAC pretreatment for 1 h prior to teroxirone exposure suppressed the induced apoptosis characteristics, while survival signals in A549 and H460 cell lines were recovered. The results proved that the generated ROS was associated with apoptotic cell death under the influence of teroxirone.

ROS enhanced cytochrome c release from mitochondria and DNA damage by teroxirone, in NSCLC cells. In order to investigate mitochondrial injury, immunofluorescence image analysis of cytochrome *c* release was used to reveal the extent of damage leading to apoptosis. The results demonstrated that teroxirone treatment enhanced the intensities of cytosolic cytochrome *c* and the effects were concentration-dependent in H460 (Fig. 5A and B) and A549 (Fig. 5C and D) cells
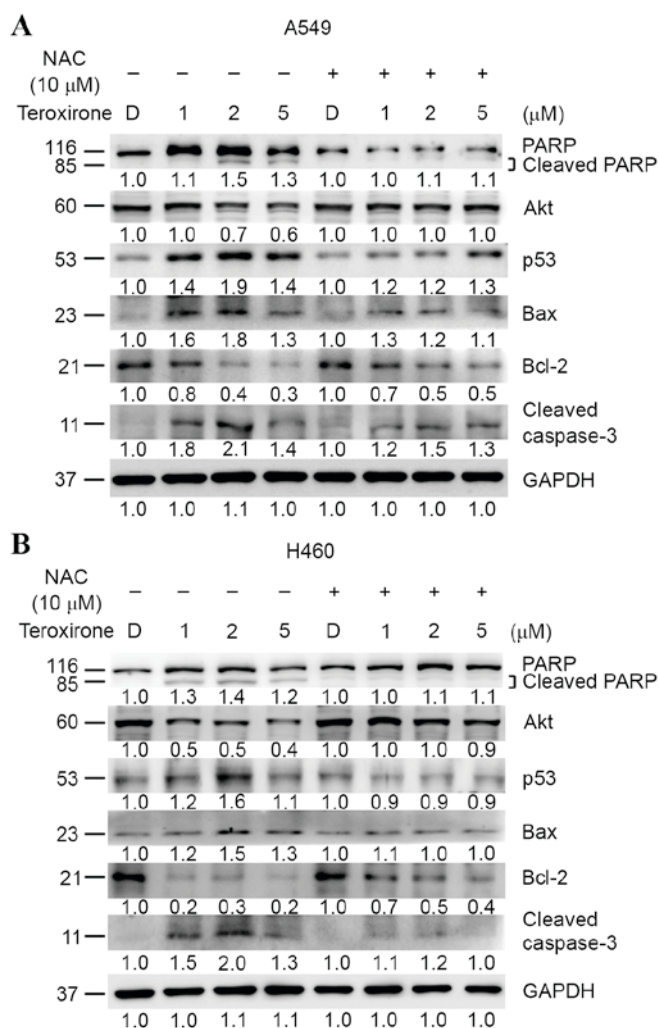
Figure 4. (A) Antioxidant NAC recovered ROS-dependent apoptosis in NSCLC A549 cells. Cells were evaluated using western blot analysis following pre-treatment with NAC (10 μM) (+) or 0.2% DMSO vehicle control (-) for 1 h, followed by various concentrations of teroxirone treatment for 24 h. The cells were lysed and the protein concentrations determined. Equal amounts of cell lysates and protein were separated by SDS-PAGE and electro-blotted. The blots were subsequently incubated in fresh blocking solution and probed for 1 h with 1:2,000 dilutions of PARP, Akt, p53, Bax, Bcl-2, caspase-3 and GAPDH antibodies, followed by incubation with a 1:3,000 dilution of a horseradish peroxidase-conjugated secondary antibody, prior to being evaluated using an ECL detection system. The numbers below each lane signified relative intensities of cleaved PARP, Akt, p53, Bax, Bcl-2 and GAPDH at each concentration compared with the results of the DMSO vehicle control with or without NAC. (B) NAC recovered ROS-dependent apoptosis in NSCLC H460 cells. Cells were analyzed by western blotting. NAC, N-acetyl cysteine; ROS, reactive oxygen species; NSCLC, non-small cell lung cancer cells; DMSO, dimethyl sulfoxide; PARP, poly ADP-ribose polymerase; Akt, protein kinase B; Bcl-2, B-cell lymphoma 2; Bax, Bcl-2-associated X protein; ECL, enhanced chemiluminescence; p53, tumor protein 53.

following treatment for 24 h. The intensity of accumulated cytochrome *c* in the cytoplasm was reduced following 1 h of NAC pretreatment. The diminished DNA lesions by teroxirone treatment, subsequent to a 24-h pretreatment with NAC in A549 cells, provided further evidence that DNA damage was resulted from generated ROS (Fig. 6). Together, these results demonstrated that ROS induced mitochondrial disturbance and DNA damage in NSCLC cells, which contributed to the effectiveness of teroxirone.
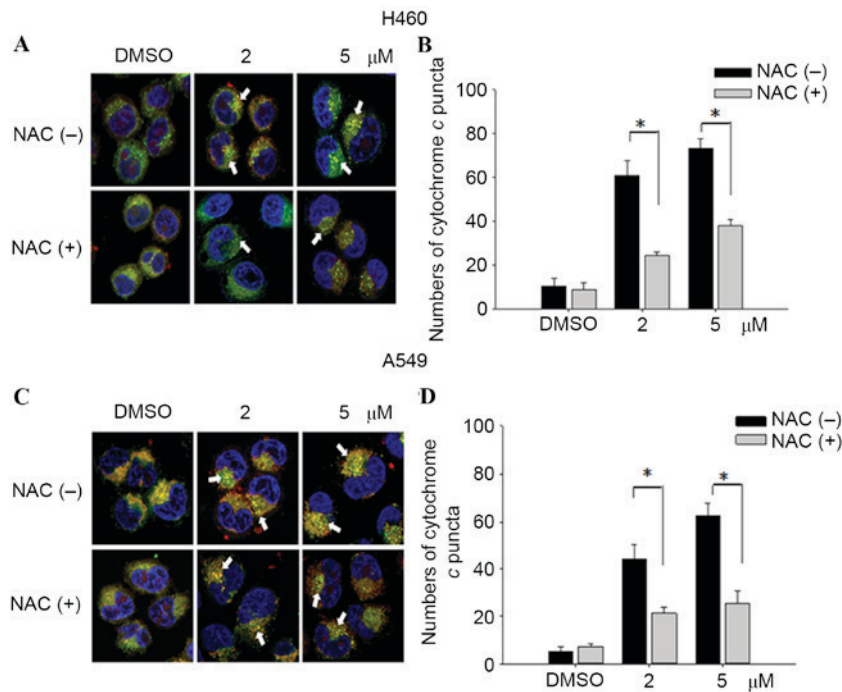
Figure 5. Cytochrome *c* release in NSCLC cells. The release of cytochrome *c* was reduced from mitochondria in H460 and A549 cells pretreated with NAC (10 μM) for 1 h, followed by incubation with 2/5 μM teroxirone or the vehicle control (0.2% DMSO) for 24 h. Cells were fixed with 4% of formaldehyde, permeabilized and stained with an anti-cytochrome *c* antibody (dilution, 1:200) at 4°C for 18 h. Subsequent to washing, cells were stained with Mitotracker Green (mitochondrial staining), DAPI (nuclear staining) and secondary antibody conjugated with TRITC for cytochrome *c*. The pointed arrow signified the co-localization of cytochrome *c* (red) and mitochondria (green), whereas the nucleus is stained blue (scale bar, 100 μm). The release of cytochrome *c* punctae was quantified in H460 (A and B) and A549 (C and D) cells using ImageJ software. The results in the presence of NAC (+) and absence NAC (-) were compared. *P<0.05 vs. DMSO control. ROS, reactive oxygen species; NSCLC, non-small cell lung cancer cells; TRITC, tetramethylrhodamine; NAC, N-acetylcysteine; DMSO, dimethyl sulfoxide.
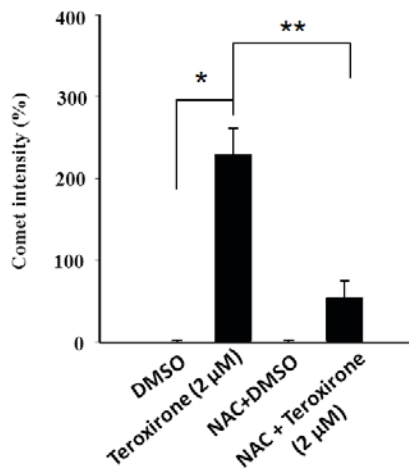

Figure 6. Relative scores of DNA damage by teroxirone in A549 cells. Mean values of the average of comet intensities for the three fields in A549 cells, which were pre-treated with NAC (10 μM) for 1 h and followed by 2 μM teroxirone or the vehicle control DMSO for 24 h, were calculated. The relative scores of the average comet intensities were obtained by converting tail intensities of the DNA tails in cells treated with 5 μM of teroxirone for 24 h and compared with those of the DMSO control. Data represented three independent experiments of the mean values ± standard deviation. *P<0.05, compared with DMSO treatment. **P<0.01, compared with NAC pretreatment. DMSO, dimethyl sulfoxide; NAC, N-acetylcysteine.

Discussion

In response to disruption of electron transport, MMP loss, ATP level decrease, ROS production and mitochondria signal transducer activation contributed to p53-dependent apoptosis (8), suggesting that the mitochondrion-dependent pathway serves a crucial role in ROS-mediated apoptosis. The increased levels of ROS may result from oxidative phosphorylation uncoupling, hyperbaric O_2 treatment, ischemia and alterations of mitochondrial lipids (9).

It has been previously revealed that teroxirone induced apoptosis in human NSCLC cells, and that this development depended on the status of p53 (6). Activation of p53 promoted the intrinsic apoptosis pathway by triggering permeabilization of the outer mitochondrial membrane and coordinating pro-apoptotic Bax and anti-apoptotic Bcl-2 (10). This process involved cytochrome *c*, mitochondrial lipids, proteins regulating bio-energetic metabolic flux and the components within the permeability transition pore (9,10). Once the outer mitochondrial membrane was disrupted, a set of proteins between the inner and outer mitochondrial membranes became active and promoted cytochrome *c* release (8). The activated intrinsic pathway was crucial in initiating apoptotic cell death under the influence of ROS (11). The released cytochrome *c* forms a cytochrome *c*/apoptotic protease activating factor 1/caspase-9 apoptosome complex, as recruited during apoptosis progression and included Bax and the initiator caspase-9 (12). Subsequently, caspase-3 and -7 was activated, causing the activation of caspase-3 downstream substrates which are critical to apoptosis (12).

The results of the present study demonstrated that teroxirone exerted oxidative stress on human NSCLC cells by disrupting the MMP, generating ROS and promoting ultimate
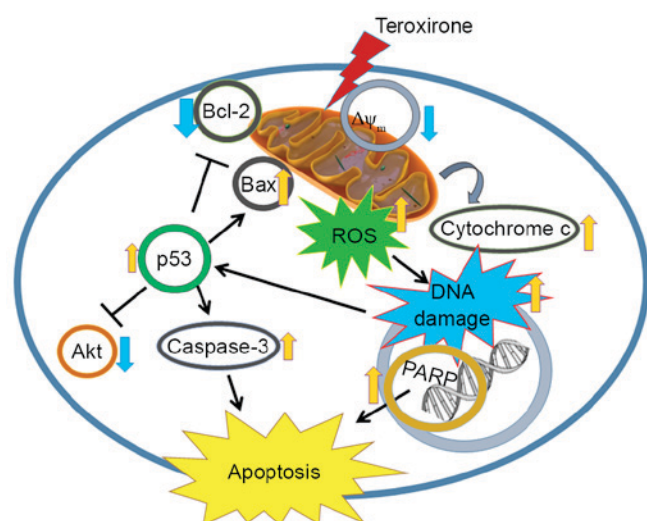
Figure 7. Molecular mechanism representation by which ROS assists apoptosis by inducing DNA damage in human NSCLC cells. Teroxirone sensitizes p53-dependent NSCLC cells to apoptosis via ROS-inducing mechanisms. ROS, reactive oxygen species; NSCLC, non-small cell lung cancer cells; Akt, protein kinase B; Bcl-2, B-cell lymphoma 2; Bax, Bcl-2-associated X protein. p53, tumor protein 53; PARP, poly ADP-ribose polymerase; $\Delta\Psi_m$, mitochondrial membrane potential.

apoptotic cell death. The decrease of the MMP was identified 12 h following teroxirone treatment, the increase of ROS 18 h following treatment and DNA damage subsequent to this. Furthermore, pretreatment with NAC significantly restored MMP (Fig. 1) and reduced ROS accumulation (Fig. 2). As demonstrated by the cell viability determination, teroxirone inhibited the proliferation of H460 and A549 cells following 24 h of teroxirone treatment. Pretreatment with NAC recovered cell growth rates and suppressed the effects of teroxirone. The decreased cell viability and the emergent sub-G_1 and G_2/M cell phase populations by teroxirone was blocked by NAC pretreatment (Fig. 3). Western blot analysis demonstrated that teroxirone induced apoptosis by increasing the expression levels of p53 and Bax, activating procaspase-3 and PARP fragmentation in addition to reducing the expression levels of Bcl-2 following 24 h of treatment (Fig. 4). Teroxirone treatment resulted in a significant increase in Bax expression and a decrease in Bcl-2 expression. A direct association exists between ROS and PI3K/Akt signal inactivation, in which ROS functions as an upstream modulator of Akt (13). The reduced Akt expression level due to teroxirone and reverted by NAC suggested the role of ROS in attenuating the PI3k/Akt signaling pathway that contributed to drug potency (14). Furthermore, the presence of NAC abolished the intrinsic pathway by suppressing p53 and Bax, in addition to decreasing caspase-3 and PARP fragmentation. In immunofluorescence analysis, NAC was revealed to block the release of cytoplasmic cytochrome *c* accumulation by teroxirone (Fig. 5). These combined results suggested the existence of teroxirone-induced ROS mediated cytotoxicity in human NSCLC cells associated with ROS. Antioxidant NAC pretreatment blocked the inhibitory effects of teroxirone by attenuating ROS (Fig. 4). Pretreatment with NAC reversed the expression of Bax, Bcl-2 and cytochrome *c*, and also inhibited teroxirone-induced MMP collapse, suggesting that

ROS was capable of functioning as an initial mediator in the p53-dependent mitochondrial apoptotic pathway. These results also support the notion that ROS serves a primary role in triggering apoptosis by activating the intrinsic pathway. Thus, as a promising potential therapy to treat NSCLC lung cancer, teroxirone affected cellular oxidative stress prior to final apoptosis.

Certain triepoxide compounds demonstrated antitumor activities against lung cancer and previous studies have identified that the triepoxide diterpenoid triptolide, as a major bioactive component of the Chinese herb, and its water-soluble analog, minnelide, promoted apoptosis and decreased proliferation in human NSCLC cells (15,16). Triptolide is an inhibitor of RNA polymerase activity and affects the transcriptional machinery. A previous study identified that the compound promoted ROS, decreased MMP and activated caspase-3 by disturbing mitochondrial functions (17). The epoxide analog benzo(a)pyrene-7,8-diol-9,10-epoxide mediated apoptosis by activating the caspase-9-dependent mitochondria pathway and the formation of ROS, loss of MMP and upregulation of p53, in human bronchiolar epithelial cells (18). The present study revealed that the triepoxide teroxirone induced apoptosis via the p53-associated intrinsic apoptosis pathway, which involves the production of ROS, the decline of MMP with implication of mitochondrial function injury and DNA damage (Fig. 7). The study provides a novel perspective of teroxirone in providing drug development and therapy for the treatment of lung cancer.

Acknowledgements

References

1. Rathos MJ, Khanwalkar H, Joshi K, Manohar SM and Joshi KS: Potentiation of in vitro and in vivo antitumor efficacy of doxorubicin by cyclin-dependent kinase inhibitor P276-00 in human non-small cell lung cancer cells. BMC Cancer 13: 29, 2013.
2. Erridge SC, Møller H, Price A and Brewster D: International comparisons of survival from lung cancer: Pitfalls and warnings. Nat Clin Pract Oncol 4: 570-577, 2007.
3. Charoensinphon N, Qiu P, Dong P, Zheng J, Ngauv P, Cao Y, Li S, Ho CT and Xiao H: 5-Demethyltangeretin inhibits human nonsmall cell lung cancer cell growth by inducing G2/M cell cycle arrest and apoptosis. Mol Nutr Food Res 57: 2103-2111, 2013.
4. Spreafico F, Atassi G, Filippeschi S, Malfiore C, Noseda S and Boschetti D: A characterization of the activity of alpha-1,3,5-triglycidyl-s-triazinetrione, a novel antineoplastic compound. Cancer Chemother Pharmacol 5: 103-108, 1980.
5. Dombernowsky P, Lund B and Hansen HH: Phase-I study of alpha-1,3,5-triglycidyl-s-triazinetrione (NSC 296934). Cancer Chemother Pharmacol 11: 59-61, 1983.
6. Wang JP, Lin KH, Liu CY, Yu YC, Wu PT, Chiu CC, Su CL, Chen KM and Fang K: Teroxirone inhibited growth of human non-small cell lung cancer cells by activating p53. Toxicol Appl Pharmacol 273: 110-120, 2013.
7. Okon IS, Coughlan KA, Zhang M, Wang Q and Zou MH: Gefitinib-mediated reactive oxygen species (ROS) instigates mitochondrial dysfunction and drug resistance in lung cancer cells. J Biol Chem 290: 9101-9110, 2015.
8. Brodská B and Holoubek A: Generation of reactive oxygen species during apoptosis induced by DNA-damaging agents and/or histone deacetylase inhibitors. Oxid Med Cell Longev 2011: 253529, 2011.

9. Simon HU, Haj-Yehia A and Levi-Schaffer F: Role of reactive oxygen species (ROS) in apoptosis induction. Apoptosis 5: 415-418, 2000.
10. Fulda S and Debatin KM: Extrinsic versus intrinsic apoptosis pathways in anticancer chemotherapy. Oncogene 25: 4798-4811, 2006.
11. Ricci JE, Muñoz-Pinedo C, Fitzgerald P, Bailly-Maitre B, Perkins GA, Yadava N, Scheffler IE, Ellisman MH and Green DR: Disruption of mitochondrial function during apoptosis is mediated by caspase cleavage of the p75 subunit of complex I of the electron transport chain. Cell 117: 773-786, 2004.
12. Herrera B, Alvarez AM, Sánchez A, Fernández M, Roncero C, Benito M and Fabregat I: Reactive oxygen species (ROS) mediates the mitochondrial-dependent apoptosis induced by transforming growth factor (beta) in fetal hepatocytes. FASEB J 15: 741-751, 2001.
13. Xu H, Li X, Ding W, Zeng X, Kong H, Wang H and Xie W: Deguelin induces the apoptosis of lung cancer cells through regulating a ROS driven Akt pathway. Cancer Cell Int 15: 25, 2015.
14. Cantley LC: The phosphoinositide 3-kinase pathway. Science 296: 1655-1657, 2002.
15. Rousalova I, Banerjee S, Sangwan V, Evenson K, McCauley JA, Kratzke R, Vickers SM, Saluja A and D'Cunha J: Minnelide: A novel therapeutic that promotes apoptosis in non-small cell lung carcinoma in vivo. PLoS One 8: e77411, 2013.
16. Reno TA, Kim JY and Raz DJ: Triptolide inhibits lung cancer cell migration, invasion and metastasis. Ann Thorac Surg 100: 1817-1825, 2015.
17. Vispé S, DeVries L, Créancier L, Besse J, Bréand S, Hobson DJ, Svejstrup JQ, Annereau JP, Cussac D, Dumontet C, et al: Triptolide is an inhibitor of RNA polymerase I and II-dependent transcription leading predominantly to down-regulation of short-lived mRNA. Mol Cancer Ther 8: 2780-2790, 2009.
18. Sang H, Zhang L and Li J: Anti-benzopyrene-7,8-diol-9,10-epoxide induces apoptosis via mitochondrial pathway in human bronchiolar epithelium cells independent of the mitochondria permeability transition pore. Food Chem Toxicol 50: 2417-2423, 2012.